

# Quantum coherence and entanglement in the avian compass: Supplementary Material

Erik Gauger,<sup>1</sup> Elisabeth Rieper,<sup>2</sup> John J. L. Morton,<sup>1,3</sup> Simon C. Benjamin,<sup>2,1</sup> and Vlatko Vedral<sup>2,3,4</sup>

<sup>1</sup>

0.25 -

-

0.25 -

-

FIG. 1: Results for a disc-shaped HF tensor. The graph on the left is precisely analogous to Fig. 2 of the main text, showing angular dependence of the singlet yield in the presence of the oscillatory field for different decay rates  $k$ . The graph on the right corresponds to Fig. 3 of the main paper, showing angular dependence of the singlet yield in the presence of environmental

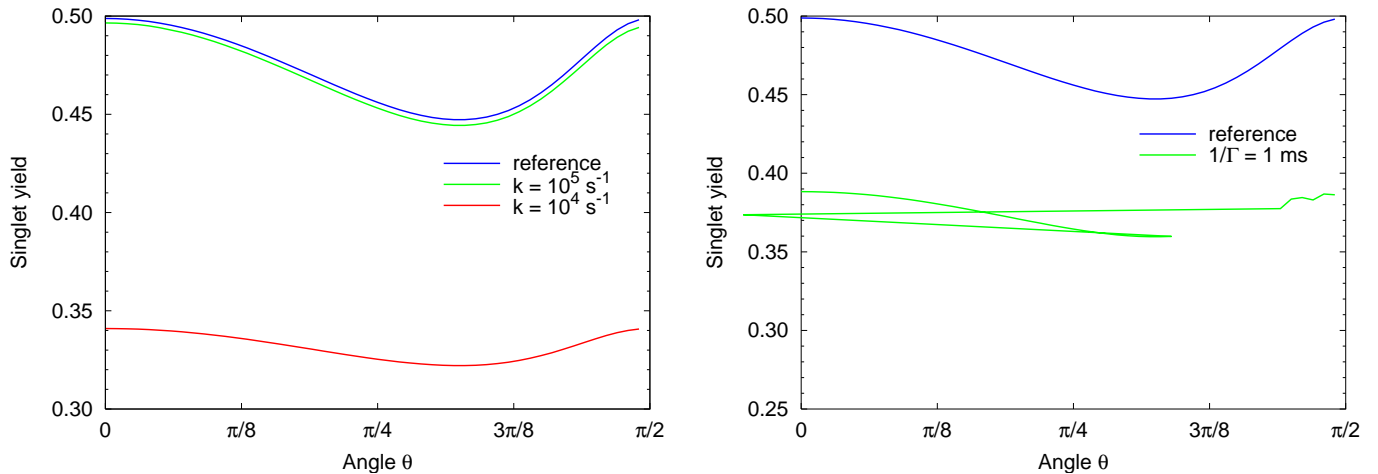


FIG. 2: Results for a model in which an anisotropic g-factor replaces the role of the nucleus to break the RP symmetry. The graph on the left is precisely analogous to Fig. 2 of the main text, showing angular dependence of the singlet yield in the presence of the oscillatory field for different decay rates  $k$ . The graph on the right corresponds to Fig. 3 of the main paper, showing angular dependence of the singlet yield in the presence of environmental noise for different noise rates  $\Gamma$ . Although the curve shapes differ, remarkably the levels of contrast remain similar to those of the conventional model in the main paper.

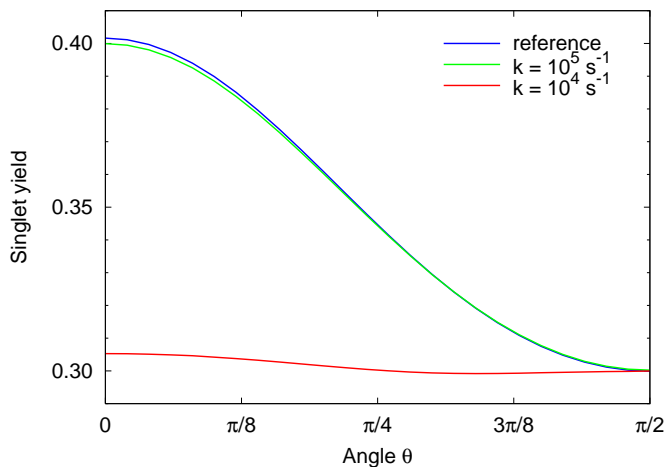


FIG. 3: Results for two nuclear spins coupled to electron 1. The graph on the left is precisely analogous to Fig. 2 of the main text, showing angular dependence of the singlet yield in the presence of the oscillatory field for different decay rates  $k$ . The graph on the right corresponds to Fig. 3 of the main paper, showing angular dependence of the singlet yield in the presence of environmental noise for different noise rates  $\Gamma$ . Although the curve shapes differ somewhat, nevertheless the parameters corresponding to serve degradation remain the same as those in the main paper ( $k = 10^4 \text{ s}^{-1}$ ,  $\Gamma = 100 \text{ s}$ ).

but gives less overall signal contrast (even in the unperturbed) scenario. We present results for these parameters in Fig. 2, confirming that the qualitative behaviour is still the same under these assumptions.

### RP pair model with two nuclear spins

In the model described in the main paper, there is a single nuclear spin coupled to one of the electrons. However, previous publications have studied the case where more than one nuclear spin is present [1, 3, 4]. Therefore, it is interesting to check whether the addition of a nuclear spin will alter our conclusions. The Hamiltonian now gains an additional coupling term,

$$H = \hat{I}_1 \cdot \mathbf{A}_1 \cdot \hat{S}_1 + \hat{I}_2 \cdot \mathbf{A}_2 \cdot \hat{S}_1 + \mathbf{B} \cdot (\hat{S}_1 + \hat{S}_2);$$

where  $\mathbf{A}_1$  is the HF tensor of the main text and  $\mathbf{A}_2 = 2-3\mathbf{A}_1$ . Here we choose a second rugby shaped HF tensor oriented parallel to the first. Note that we have also considered different relative coupling strengths and geometries (such as a pancake shaped and rugby shaped tensor), but again, these choices do not influence our core conclusions. Results for the particular choice of parameters described above are shown in Fig. 3.

### PURE DEPHASING NOISE MODEL

Interestingly, if we begin the simulation with a completely dephased state:  $(j_s i h s j + j t_0 i h t_0 j) = 2$ , the classical correlations are still sufficient for achieving adequate angular visibility and neither quantum phase coherence nor entanglement seems to be a prerequisite for the efficiency of the avian compass.

To explore this idea further, we would like to study 'pure dephasing' occurring *during* the singlet-triplet interconversion. In essence we use energy conserving noise operators, Eqn. (1), which are known to be the dominant source of decoherence in so many other artificially made quantum systems. By applying this specific noise, we confirm that the compass mechanism's performance is essentially immune, while of course the coherence of the quantum state of the electrons would be degraded.

One might be inclined to conclude that, if pure dephasing noise is indeed dominant, then the avian compass need not protect quantum coherence for the long time scales suggested in the main paper. But crucially, we also show that if such noise were naturally present at a high level in the compass (exceeding the generic noise level by more than an order of magnitude) then it would render the bird immune to the weak oscillatory magnetic fields studied by Ritz *et al.* [1]. Thus the sensitivity to oscillatory fields implies that both amplitude and phase, and thus entanglement, are indeed protected within the avian compass on timescales exceeding tens of microseconds.

Since the electron spin singlet state is not an eigenstate of the Hamiltonian, the dephasing operators will be different from the ones mixing the phase of the singlet and triplet state within the electronic subspace. Instead, we replace the previously defined noise operators of  $L_i$  of Eq. (3) by appropriate dephasing operators as follows: we treat the remote electron and the electron nuclear spin subsystem separately. Within both subsystems, we define dephasing operators

$$Z_i = \frac{1}{2} \sum_{j \in i} \left( j_j i h j j + j_j i h j j \right) A = \frac{1}{2} (I_4 - 2j_j i h j j); \quad (1)$$

where  $f_j, i g$  are the set of normalised eigenvectors of this subsystem. This results in two dephasing operators for the remote electron (these can be combined to a single  $Z_z$  operator rotated with the field) and four operators for the electron nuclear spin subsystem. Each of these dephasing operators corresponds to fluctuations of one of the (subsystem's) energy levels.

Strikingly, the singlet yield is entirely unaffected by this particular kind of noise, i.e. it is entirely independent of the dephasing rate  $\gamma_z$ . Thus, a curve obtained with this model coincides perfectly with the reference curve of Fig. 3 of the main paper. However, we show in the following that the dephasing rate of this model can be at most ten times faster than the generic noise rate to retain sensitivity to the oscillatory field.

Fig. 4 shows the singlet yield as a function of  $\gamma$  for different pure dephasing rates  $\gamma_z$ . Pure phase noise would actually *protect* the compass from the harmful effect of an applied oscillatory field (by suppressing the Rabi oscillations caused by such a field). We see that an aggressive pure dephasing rate of  $\gamma_z = 10 \gamma$  almost completely recovers the reference curve (corresponding to a noise-free system without oscillatory field).

### OSCILLARECOVERST

(  $\gamma_z = 10 \gamma$  ) ( coherence ) - 34 % ( migh ) 28 (  $\gamma$  ) - 34 % ( e ) - 333 ( el 28 )





above with the 'dotted line picture' some level of Markovian noise will also be inevitably present on the long timescale required for the RP process, thus we are still dealing with a computationally demanding open systems problem, limiting the number of spins that can be simulated.

Figure 6 shows results obtained for a RP model consisting of two electron and four nuclear spins. As before, one of the nuclear spins is a central part of the mechanism through its anisotropic coupling to electron 1 with parameters as in the main paper. The remaining three nuclear spins serve as an additional local spin bath, and we have assumed isotropic hyperfine coupling strengths of  $A_2 = A_z=8$ ;  $A_3 = A_z=10$ ;  $A_4 = A_z=12$  with electron 1 ( $A_z = 10^{-5}$  meV). All nuclear spins are initialised in a fully mixed state as appropriate for a room temperature environment. The presence of the additional nuclear spins introduces some ripples into the shape of the curves, yet there is no qualitative difference with regard to the effects of irreversible noise and the oscillatory field. This means that we must once more arrive at the same conclusion that the compass system is remarkably well protected from an irreversible loss of coherence. We note that further calculations with only three protons and for a range of different coupling strengths (not shown) display the same qualitative behaviour, indicating that there is no trend for an increasing number of spins that would alter our conclusion.

## ADDITIONAL NOISE MODELS

Having simultaneously considered all 63 processes, we now look at the effect of individual Lindblad operators. We focus on the nine subsets of operators which affect coherence on *both* electron spins (otherwise the coherence time of at least one part of the compass would be infinite). Summing over the four possible nuclear combinations, we obtain the manageable number of nine noise models, each with isotropic noise on the nuclear spin [5].

All curves in our calculations have the same shape with the largest singlet yield achieved for  $\theta = 0$  and the lowest singlet yield in the perpendicular configuration  $\theta = \pi/2$ . The difference in singlet yield between those two configurations corresponds to the signal contrast and is a good measure for judging the performance of the compass. In the absence of noise and the oscillatory field, the contrast is  $0.382 - 0.281 = 0.101$ , and we shall use this value as the benchmark for comparing the different noise models.

Noise model	1= = 100 s			1= = 10 s		
	Noise [%]	Noise & RF [%]	Degradation [%]	Noise [%]	Noise & RF [%]	Degradation [%]
general noise	14.49	13.98	3.54	1.65	1.649	0.05
$x \otimes x$	39.09	34.55	11.62	5.85	5.83	0.23
$x \otimes y$	40.45	35.78	11.55	6.05	6.03	0.23
$x \otimes z$	12.72	11.61	8.73	1.42	1.41	0.16
$y \otimes x$	40.45	35.82	11.46	6.05	6.03	0.23
$y \otimes y$	39.09	34.59	11.51	5.84	5.83	0.23
$y \otimes z$	11.36	10.42	8.26	1.21	1.21	0.16
$z \otimes x$	12.72	12.24	3.77	1.42	1.42	0.05
$z \otimes y$	11.36	11.02	3.02	1.21	1.21	0.03
$z \otimes z$	39.09	35.98	7.97	5.84	5.83	0.15
pure dephasing	99.999	63.45	36.55	99.991	92.41	7.58
match experiment	high	strongly reduced	high	high	strongly reduced	high

TABLE I: Contrast for the nine different Lindblad operators compared to the isotropic noise model of the main paper and the pure dephasing noise. The "Noise model" column specifies the type of noise and for the  $i \otimes j$  entries  $i$  and  $j$  are the noise acting on the 'local' and 'remote' electron spin respectively. The "Noise" and "Noise & RF" columns give the signal contrast as a percentage of the ideal unperturbed system (see text). The \u0001141..855 401..855 44 J 0.398 w 0 0 m 490.837 0 | S Q BT /F15



- [2] I.A. Solov'yov, D. E. Chandler, K. Schulten: *Magnetic Field Effects in Arabidopsis thaliana Cryptochrome-1*, Biophysical Journal, **92**, 2711-2726 (2007).
- [3] C. T. Rodgers, P.J. Hore: *Chemical magnetoreception in birds: The radical pair mechanism*, PNAS, **106** 2, 353-360, (2009).
- [4] C.T. Rodgers: *Magnetic Field Effects in Chemical Systems*, PhD Thesis, Oxford (2007).
- [5]